



# Waste ashes as catalysts for the pyrolysis–catalytic steam reforming of biomass for hydrogen-rich gas production

Amal S. Al-Rahbi<sup>1</sup> · Paul T. Williams<sup>1</sup>

Received: 19 November 2018 / Accepted: 21 May 2019 / Published online: 24 May 2019  
© The Author(s) 2019

## Abstract

Combustion ashes from coal, refuse-derived fuel (RDF) and waste tyres have been investigated as potential catalysts for the production of a hydrogen-rich gas from waste biomass. The process used a two-stage reactor involving pyrolysis of the biomass followed by catalytic steam reforming of the evolved pyrolysis gases using the ash catalysts. The ashes were also impregnated with 10 wt% nickel to determine the influence on hydrogen production. In the presence of the ash samples, the total gas yield and hydrogen yield significantly increased, particularly for the refuse-derived ash. The ash samples contained a high metal content, including Al, Ca, Mg, Cu and Fe, K, Na and Zn. All such metals have been reported to act as catalysts for hydrogen production. In the absence of catalyst, the total gas yield from the biomass was 39.9 wt% which increased to 52.7 wt% with the tyre rubber ash, to 50.3 wt% with coal ash and 59.5 wt% with RDF ash. The highest hydrogen yield of 7.90 mmol g<sup>-1</sup> biomass was produced in the presence of the RDF-derived ash, representing 29.73 vol% H<sub>2</sub>. Addition of nickel to the combustion ash samples showed a further significant increase of ~20% in the yield of hydrogen.

**Keywords** Biomass · Pyrolysis · Reforming · Waste · Ash

## Introduction

The range of fuels used in combustion systems for the generation of power has expanded from the combustion of coal in power plants, to include the use of a variety of waste materials [1]. For example, municipal solid waste and refuse-derived fuels combusted for energy recovery in waste to energy plants, biomass forestry residues for large and smaller scale power production and waste tyres to provide the energy in cement kilns. However, the combustion process generates a residual ash which may be produced in large quantities. For example, it is estimated that 750 Mt of coal ash are produced world-wide each year [2] and ~100 million tonnes per year in the EU [3]. Incineration of municipal solid waste in waste to energy plants generates approximately 25 wt% of bottom ash consisting of more than 90% bottom ash and ~10% fly ash and air pollution control residues. Bottom ash is regarded as inert, but fly ash and pollution control residues are hazardous. It has been estimated that approximately

18 million tonnes of bottom ash is produced in the EU each year [4].

Often the residual ash from coal combustion or municipal solid waste incineration is deposited in waste landfill sites. However, there is current interest in the sustainable management of waste ashes to maximise the recovery of resources. Residual combustion ashes have been investigated for use as alternative products [1]. For example, coal ash has been processed for use in the production of bricks [5], for use in concrete [6] and for cement production [7]. The ash residue from the incineration of municipal solid waste has been used in the production of light weight aggregate material [8] and also incorporated in asphalt mixtures for paving material [9] and in cement composites [10].

The ash produced from the combustion of the solid hydrocarbon fuels, coal, municipal solid waste and waste tyres contains a range of metal-based components. The main constituents in coal ash from power plants are SiO<sub>2</sub>, Al<sub>2</sub>O<sub>3</sub>, Fe<sub>2</sub>O<sub>3</sub>, CaO and MgO [2]. Goodarzi [11] reported a wide range of oxides identified in coal-fired power plant fly ash including, SiO<sub>2</sub>, Al<sub>2</sub>O<sub>3</sub>, Fe<sub>2</sub>O<sub>3</sub>, TiO<sub>2</sub>, P<sub>2</sub>O<sub>5</sub>, CaO, MgO, SO<sub>3</sub>, Na<sub>2</sub>O, K<sub>2</sub>O, BaO, SrO, V<sub>2</sub>O<sub>5</sub>, NiO, MnO and Cr<sub>2</sub>O<sub>3</sub>. Lynn et al. [12] reported that the composition of municipal solid waste incinerator bottom ash comprised largely, SiO<sub>2</sub>, CaO

✉ Paul T. Williams  
p.t.williams@leeds.ac.uk

<sup>1</sup> School of Chemical and Process Engineering, University of Leeds, Leeds LS2 9JT, UK

and  $\text{Al}_2\text{O}_3$ , with others oxides at lower concentrations identified as  $\text{Fe}_2\text{O}_3$ ,  $\text{Na}_2\text{O}$ ,  $\text{MgO}$ ,  $\text{SO}_3$ ,  $\text{P}_2\text{O}_5$ ,  $\text{ZnO}$  and  $\text{CuO}$ . A detailed compositional analysis of incinerator bottom ash showed the presence of various silicates, oxides and carbonates, such as,  $\text{Ca}_2\text{Al}_2\text{SiO}_7$ ,  $\text{Ca}_2\text{MgSi}_2\text{O}_7$ ,  $\text{SiO}_2$ ,  $\text{Fe}_3\text{O}_4$ ,  $\text{Fe}_2\text{O}_3$ ,  $\text{CaCO}_3$ ,  $\text{MgCO}_3$ ,  $\text{Ca}(\text{OH})_2$ ,  $\text{CaSO}_4$ ,  $\text{NaCl}$  and  $\text{KCl}$  and elemental  $\text{Fe}$ ,  $\text{Al}$  and  $\text{Cu}$  [13]. Species identified in waste incinerator fly ash include,  $\text{Pb}_3\text{SiO}_5$ ,  $\text{Pb}_3\text{O}_2\text{SO}_4$ ,  $\text{Pb}_3\text{Sb}_2\text{O}_7$ ,  $\text{PbSiO}_4$ ,  $\text{Cd}_5(\text{AsO}_4)_3\text{Cl}$ ,  $\text{CdSO}_4$ ,  $\text{K}_2\text{ZnCl}_4$ ,  $\text{ZnCl}_2$ ,  $\text{ZnSO}_4$ ,  $\text{Fe}_3\text{O}_4$ ,  $\text{Fe}_2\text{O}_3$ ,  $\text{SiO}_2$ ,  $\text{CaSiO}_3$ ,  $\text{Al}_2\text{SiO}_5$ ,  $\text{Ca}_3\text{Si}_3\text{O}_9$ ,  $\text{CaAl}_2\text{SiO}_6$ ,  $\text{Ca}_3\text{Al}_6\text{Si}_2\text{O}_{16}$ ,  $\text{NaAlSi}_3\text{O}_8$ , and  $\text{KAlSi}_3\text{O}_8$  [14]. Singh et al. [15] reported that the main constituents of the ash produced from waste tyre rubber combustion comprises,  $\text{SiO}_2$ ,  $\text{Al}_2\text{O}_3$  and  $\text{ZnO}$  with much lower ( $< 2.5$  wt%) concentrations of  $\text{Fe}_2\text{O}_3$ ,  $\text{K}_2\text{O}$ ,  $\text{CaO}$ ,  $\text{TiO}_2$ ,  $\text{MgO}$ ,  $\text{Na}_2\text{O}$  and  $\text{P}_2\text{O}_5$ .

The high metal content in such wastes indicates that the ash has the potential to be used as catalytic materials for a variety of applications. For example, Wang et al. [16] investigated the use of coal ash catalysts for the catalytic steam reforming of acetic acid and phenol as representative model bio-oil compounds for the production of hydrogen. They reported that the presence of metals in the ash catalysed the steam-reforming reaction, resulting enhanced carbon conversion and production of hydrogen. Shahbaz et al. [17] investigated the catalytic steam gasification of palm shell as a biomass feedstock with coal ash as a catalyst for the production of syngas and hydrogen. The optimised process conditions with the coal ash catalyst produced a hydrogen yield of 36.9 vol% and syngas yield of 61.9 vol%. They attributed the increased yield of syngas and hydrogen to the presence of  $\text{Fe}_2\text{O}_3$ ,  $\text{MgO}$ ,  $\text{Al}_2\text{O}_3$ , and  $\text{CaO}$  in the ash. Loy et al. [18] used coal ash as a catalyst for the catalytic pyrolysis of rice husks for the production of syngas. They reported that coal ash catalysed the production of hydrogen and syngas compared to non-catalytic pyrolysis, producing 68.3 vol% syngas and also enhancing the hydrogen content of the syngas by 8.4 vol%.

Incinerator bottom ash has been used as a catalyst for the cracking of tars produced from the gasification of municipal solid waste [19]. The tar was represented as toluene model compound and using the incinerator bottom ash catalyst, the toluene cracking conversion was 40.1% at 750 °C, which was reported to be significantly higher than that of thermal cracking. At a higher ash catalyst temperature of 950 °C the toluene conversion was 94.2%.

The analysis of the literature shows that ash derived from combustion of solid fuels possesses catalytic properties for several applications. The motivation for the work presented here was to expand this knowledge to investigate the potential of ash residues derived from the combustion of coal, refuse-derived fuel (RDF) and waste tyre rubber to act as catalysts for the catalytic steam reforming of biomass pyrolysis gases. A two-stage reactor has been used, whereby

the first stage involves pyrolysis of biomass and the product pyrolysis gases are then passed directly to a catalytic steam-reforming reactor containing the combustion ashes. The gases from the process have been analysed in detail with the aim of maximising the production of a hydrogen-rich gas.

## Materials and methods

### Materials

Waste wood pellets with a particle size of 1 mm were used as the biomass feedstock for pyrolysis reforming/steam gasification experiments. The wood pellets were produced as compressed saw dust pellets from waste wood processing by Liverpool Wood Pellets Ltd, Liverpool, UK. The proximate analysis of the wood pellets gave 75.0 wt% volatiles, 7.0 wt% moisture, 2.0 wt% ash, and 15.0 wt% fixed carbon. Elemental analysis gave 46.0 wt% carbon, 5.6 wt% hydrogen, 0.7 wt% nitrogen and 45.7 wt% oxygen (by difference).

Ash samples derived from coal, waste tyre and RDF were used as a catalyst for gas and hydrogen production during the biomass pyrolysis–catalytic steam-reforming process. The coal, waste tyre and RDF were ashed in a furnace at 700 °C for 4 h. The produced ash samples were further examined as a catalyst support using an impregnation method to produce Ni-ash catalysts. For this purpose, the coal, waste tyre, and RDF ash samples were impregnated with nickel using an aqueous solution of  $\text{Ni}(\text{NO}_3)_2 \cdot 6\text{H}_2\text{O}$  (corresponding to Ni loading of 10 wt%). The mixture of ash and  $\text{Ni}(\text{NO}_3)_2 \cdot 6\text{H}_2\text{O}$  was stirred using a magnetic stirring apparatus at 100 °C to produce a slurry, dried overnight and calcined followed by calcination at 750 °C for 3 h in an air atmosphere. Finally, the obtained catalysts were reduced at 800 °C under hydrogen.

### Characterization of the produced ash catalysts

The composition of the ash samples was determined using a Thermo Advant XP X-ray fluorescence (XRF) spectrometer. The samples were prepared as fused beads to provide a homogenous sample. A lithium borate flux was added to the ash samples and heated to 900 °C in a platinum crucible and then cast into a mould. The resultant fused bead was presented to the XRF spectrometer for analysis. The fused bead was analysed using OXSAS programme. The surface area of the produced coal, waste tyre and RDF ash samples was determined according to the Brunauer–Emmet–Teller (BET) method using a Quantachrome NOVA 2200e series apparatus. Samples were degassed at 250 °C for 3 h under vacuum prior to measurement. A Bruker D-8 diffractometer with  $\text{Cu K}\alpha$  radiation operated at 40 kV and 40 mA was used to obtain the X-ray diffraction (XRD) patterns of the original

product ash samples and the nickel-supported ash catalysts. The XRD pattern identification was obtained using HighScore Plus software. A Hitachi SU8230 scanning electron microscope (SEM) coupled to an energy-dispersive X-ray spectrometer (EDXS) system was used to characterise and examine the surface of the tested catalysts.

## Reactor system

It is a two-stage fixed bed reactor system consisting of a first stage involving pyrolysis of the wood pellets and a second-stage catalytic reactor containing the produced residual coal, tyre and RDF ashes. A schematic diagram of the system is shown in Fig. 1. The reactors were constructed of stainless steel with an inner diameter of 22 mm and a length of 160 mm with monitoring and control of gas flow and temperature.

The experiments consisted of the initial heating of the second-stage catalytic reactor containing 1.0 g of ash catalyst to a temperature of 800 °C and maintained at that temperature throughout the experiment. In addition, water was injected into the second-stage catalytic reactor using a syringe pump at a rate of 4.0 g h<sup>-1</sup> (steam/biomass (S/B) ratio of 2). After the catalytic reactor temperature was stabilised at 800 °C, the first-stage pyrolysis reactor containing the biomass (1.0 g) was heated at a rate of 40 °C min<sup>-1</sup> to a final temperature of 600 °C. The evolved pyrolysis gases from biomass thermal degradation mixed with the steam and underwent catalytic steam reforming over the coal, tyre

and RDF ash catalysts and Ni-ash catalysts. For comparison with the ash-based catalysts, clean and washed quartz sand was used in place of the catalyst in the second-stage reactor. The sand would have none of the catalytic metals found in the ash-based catalysts. Any condensable liquid products, including condensed steam, were collected in a condenser system cooled with dry ice. Gases passing through the condenser system were collected in a Tedlar™ gas sample bag.

The product gases in the gas sample bag were analysed immediately after each experiment using three Varian CP-3380 gas chromatographs (GC). N<sub>2</sub>, H<sub>2</sub>, and CO gases were analysed using a 60–80-mesh molecular sieve packed column, Ar carrier gas and thermal conductivity detector (TCD). CO<sub>2</sub> gas was analysed on a second Varian GC with a 80–100-mesh HayeSep packed column, Ar carrier gas and TCD. CH<sub>4</sub>, C<sub>2</sub>H<sub>6</sub>, C<sub>2</sub>H<sub>4</sub>, C<sub>3</sub>H<sub>8</sub>, C<sub>3</sub>H<sub>6</sub>, C<sub>4</sub>H<sub>10</sub>, C<sub>4</sub>H<sub>8</sub> and C<sub>4</sub>H<sub>6</sub> hydrocarbon gases were analysed on a third Varian GC with an HayeSep 80–100-mesh molecular sieve column, N<sub>2</sub> as carrier gas and flame ionisation detector (FID).

## Results and discussion

### Characterization of the ash catalysts

The ash samples that were produced from the coal, waste tyre rubber and RDF and used for the pyrolysis–catalytic steam-reforming experiments were characterised using XRF, surface area analysis, XRD, and SEM. Table 1 shows the metal-oxide compositional analysis of the derived combustion ashes produced by XRF. The waste tyre rubber combustion ash is dominated by the presence of zinc which is added to the tyre vulcanisation process to improve the physical properties of the rubber. In addition, silica (SiO<sub>2</sub>) is present in high concentration, and the silica is often added as filler material for the tyre formulation. The RDF ash contains typical metal compounds that are found in waste incinerator combustion ash. RDF is prepared from municipal solid

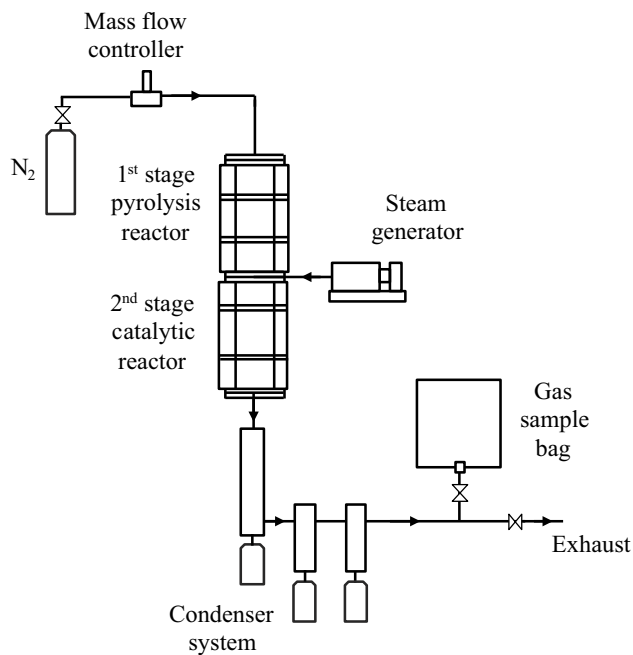


**Fig. 1** Schematic diagram of the two-stage, biomass pyrolysis–catalytic steam-reforming reactor

**Table 1** Chemical composition of the ash samples (wt%)

Sample	Tyre ash	RDF ash	Coal ash
SiO <sub>2</sub>	24.2	3.31	58.2
ZnO	41.5	0.6	–
Al <sub>2</sub> O <sub>3</sub>	2.3	21.0	20.8
CaO	3.3	16.9	2.9
MgO	0.7	4.6	1.4
CuO	0.9	0.1	–
K <sub>2</sub> O	0.9	2.5	1.7
Fe <sub>2</sub> O <sub>3</sub>	5.7	3.3	9.3
Na <sub>2</sub> O	3.0	1.9	2.3
SO <sub>3</sub>	15.5	3.03	0.9

waste with the aim of raising the calorific value of the product fuel by removing metals, glass and ceramic materials. The RDF ash prepared in this work contained mainly  $\text{Al}_2\text{O}_3$  and  $\text{CaO}$  with minor concentrations of other alkali metals. The coal ash sample consisted of mainly  $\text{SiO}_2$ ,  $\text{Al}_2\text{O}_3$  and  $\text{Fe}_2\text{O}_3$ .

Table 2 shows the surface areas and pore diameter for the ash samples and the nickel-ash catalysts. The BET surface areas of the ash samples produced from RDF, tyre rubber and coal were found to be 21.8, 13.7 and  $2.5 \text{ m}^2 \text{ g}^{-1}$ , respectively. However, nickel catalysts supported on RDF ash showed a slightly reduced surface area than the original ash samples.

The morphologies of the produced ash catalysts and Ni-ash catalysts were characterised by scanning electron microscopy (SEM) and are presented in Fig. 2. The coal ash shows the characteristic cenospheres produced during coal combustion. The tyre rubber-derived ash and RDF-derived ash show less structure. The addition of 10 wt% nickel to the ash appears to show surface deposits of the metal.

Figure 3 shows XRD profiles of the produced ash catalysts and Ni-ash catalysts. The diffraction peaks observed around  $2\text{-}\theta$   $44^\circ$  and  $52^\circ$  with the ash-supported nickel catalysts were related to the presence of metallic Ni and no peaks corresponding to the NiO phase were identified. This was expected as the catalysts were reduced before the catalytic steam-reforming process. The XRD diffraction peaks observed with Ni/tyre ash were smaller compared to the XRD peaks obtained with either Ni/coal or Ni/RDF catalysts, which might indicate that the particle size of Ni is smaller for the Ni/tyre ash sample.

### Pyrolysis–catalytic steam reforming of biomass with ash catalysts

Table 3 shows the product yield and gas composition for the pyrolysis–catalytic steam reforming of biomass with the ash-based catalysts. In addition, experiments were carried out with clean quartz sand in place of the catalyst and the results shown in Table 3 indicate that catalytic cracking and steam

reforming are taking place, even in the presence of sand. The particles of sand in the second-stage reactor is maintained at  $800^\circ\text{C}$ , producing a hot surface for thermal cracking and steam reforming of the evolved pyrolysis gases from the biomass thermal degradation. In the presence of the sand, the total gas yield in relation to the feedstock biomass was 39.9 wt% which increased to 52.7 wt% when tyre rubber ash was introduced and with coal ash and RDF ash, increased to 50.3 wt% and 59.5 wt%, respectively. The metals in the ash sample produce a catalytic effect producing more product gas, particularly for the RDF ash sample. The residual char yield derived from the biomass pyrolysis in the first-stage reactor was constant at  $\sim 19.0$  wt% for all the experiments since it was unaffected by the second-stage reactions. Consequently, the liquid yield from biomass (by difference) represented 41.1 wt% for the sand, 28.3 wt% for the tyre ash, 30.7 wt% for the coal ash and 21.5 wt% for the RDF ash. Suggesting that cracking of the higher molecular weight biomass volatile compounds to gas occurred in the presence of the ash samples compared with the non-catalytic sand.

The gas composition shown in Table 3 shows that the product gases consist of mainly  $\text{CO}$ ,  $\text{CO}_2$ ,  $\text{H}_2$ ,  $\text{CH}_4$  and  $\text{C}_2\text{H}_4$  hydrocarbons. The influence of ash addition to the catalytic reactor is to increase the level of catalytic steam reforming of the hydrocarbons ( $\text{CH}_4$  and  $\text{C}_2\text{H}_4$ ) which show a decrease in concentration compared to the non-catalytic experiment (sand) and a consequent increase in  $\text{H}_2$  production. In addition, the decrease in  $\text{CO}$  and increase in  $\text{CO}_2$  and  $\text{H}_2$ , compared to the non-catalytic (sand) results indicates that the presence of the ash enhances the water gas shift reaction. Overall, the presence of the ash with their inherent metal content acts as a catalyst for the production of hydrogen from the biomass pyrolysis gases. The highest hydrogen gas yield of 29.73 vol% representing  $7.90 \text{ mmol H}_2 \text{ g}^{-1} \text{ biomass}$  was produced in the presence of the RDF-derived ash.

Table 1 showed a high metal content in the ash, including  $\text{Al}_2\text{O}_3$ ,  $\text{CaO}$ ,  $\text{MgO}$ ,  $\text{CuO}$  and  $\text{Fe}_2\text{O}_3$ , depending on the waste ash used. During the catalytic steam-reforming process, the metal oxides would undergo reduction to the metal via the reducing gases such as hydrogen and carbon monoxide produced during the process. The metal oxides,  $\text{Al}_2\text{O}_3$ ,  $\text{CaO}$ ,  $\text{MgO}$ , and  $\text{Fe}_2\text{O}_3$ , have been used as catalysts for the catalytic steam reforming of biomass [20, 21]. Magnesium, acting as a promoter in nickel-based catalysts, has also been investigated by Garcia et al. [22] where it was reported to produce a higher hydrogen yield in the steam reforming of an aqueous fraction of bio-oil. In a later report, Garcia et al. [23] also showed that magnesium containing  $\text{NiMgAl}_2\text{O}_5$  catalyst produced high total gas and hydrogen yields for the hydrogen production from biomass catalytic steam gasification for biomass in the form of pine sawdust. The high yields of  $\text{H}_2$  and  $\text{CO}_2$  coupled with low yields to  $\text{CH}_4$ ,  $\text{C}_2$  hydrocarbons and  $\text{CO}$  suggesting high catalytic activity for

**Table 2** Surface area and porosity of the ash catalysts

Catalyst	BET surface area ( $\text{m}^2 \text{ g}^{-1}$ )	Pore diameter (nm)
RDF ash	21.8	1.239
Tyre ash	13.7	0.710
Coal ash	2.5	0.703
10 wt%Ni/RDF ash	12.8	1.713
10 wt%Ni/tyre ash	15.1	1.098
10 wt%Ni/coal ash	3.6	1.371

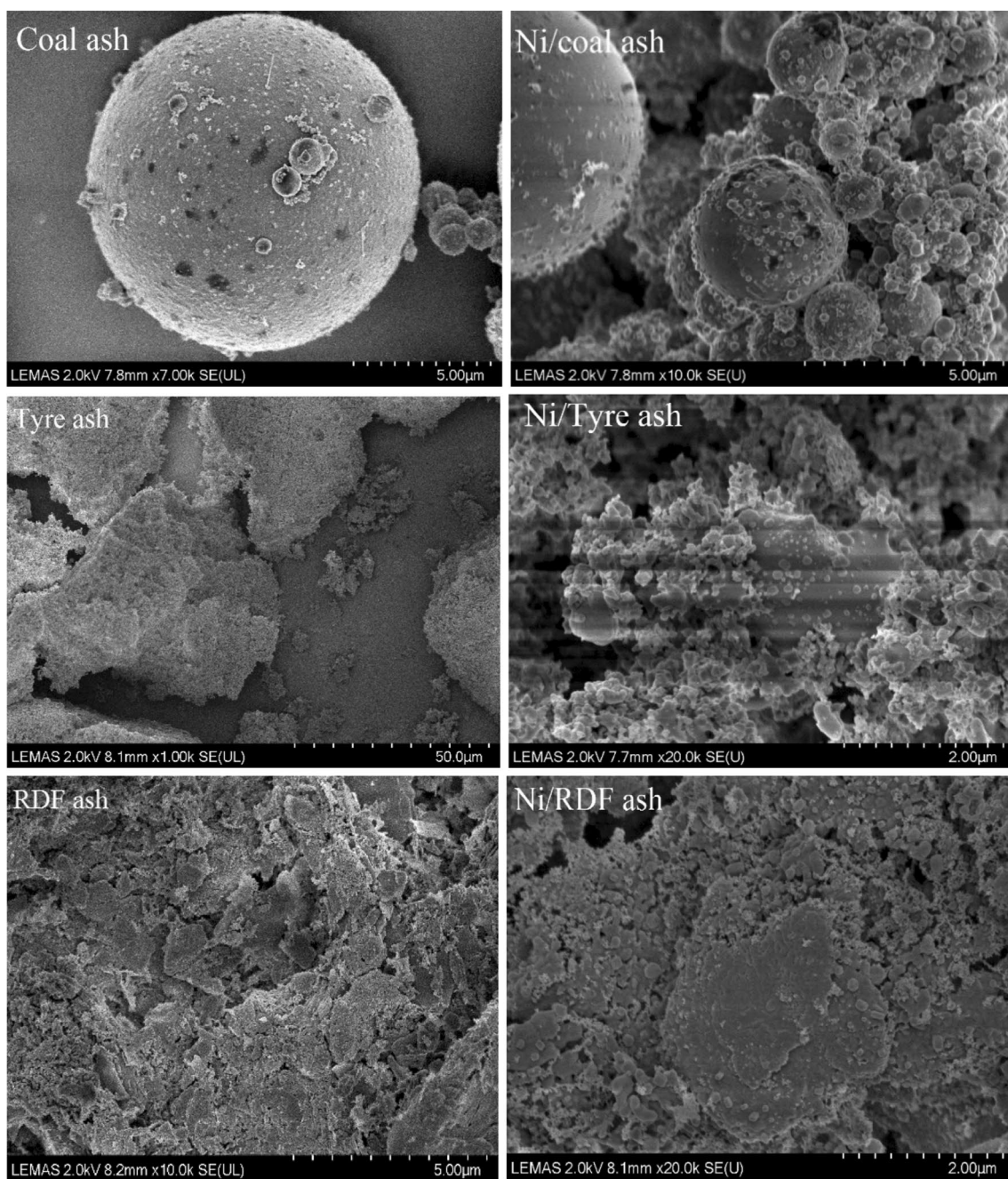


**Fig. 2** Scanning electron micrographs of the ash and Ni-ash catalysts

the steam-reforming reactions of hydrocarbons and the water gas shift reaction. The presence of copper as a Ni-catalyst promotor metal for the production of hydrogen has been shown to enhance the yield of hydrogen and decomposition of methane [24]. The addition of zinc to catalytically steam reform wood sawdust biomass pyrolysis gases using a Ni/Zn/Al<sub>2</sub>O<sub>3</sub> catalyst showed that the total gas yield and hydrogen yields were increased producing a maximum gas yield of 74.8 wt% and H<sub>2</sub> yield of 20.1 mmol H<sub>2</sub> g<sup>-1</sup> biomass [25]. In

the absence of the Ni/Zn/Al<sub>2</sub>O<sub>3</sub> catalyst, the total gas yield was only 33.0 wt% and hydrogen yield only 2.4 mmol H<sub>2</sub> g<sup>-1</sup> biomass. On the one hand, zinc modifies the surface structure and the surface chemistry of the catalysts by formation of zinc aluminates, and on the other hand, zinc oxide can be reduced to metallic zinc under reaction conditions, thus modifying the catalytic properties of the active phase. The presence of Zn increases the ethanol conversion to gaseous compounds as compared with the catalyst supported on the

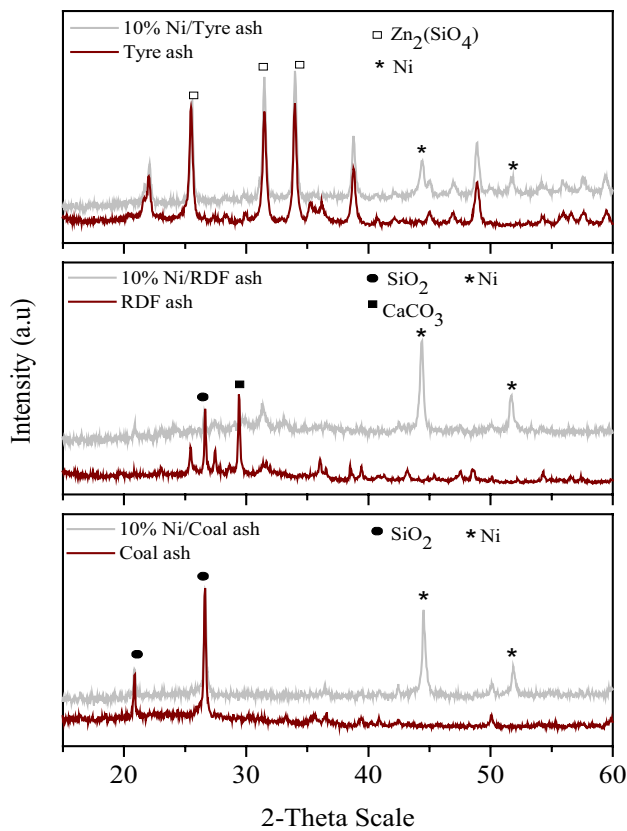


**Fig. 3** XRD analysis of the ash and Ni-ash catalysts

**Table 3** Gas yield and gas composition from the pyrolysis–catalytic steam reforming of biomass with the ash-based catalysts

Sample	Sand	Tyre ash	Coal ash	RDF ash
Gas yield (wt%)	39.9	52.7	50.3	59.5
Gas composition (vol%)				
CO	43.50	35.29	42.16	34.51
CO <sub>2</sub>	14.10	19.22	15.49	20.63
H <sub>2</sub>	19.92	27.98	22.08	29.73
CH <sub>4</sub>	15.33	12.10	14.38	10.74
C <sub>2</sub> H <sub>4</sub>	7.15	5.42	5.88	4.39
H <sub>2</sub> yield (mmol g <sup>-1</sup> biomass)	3.39	6.54	4.79	7.90

**Table 4** Gas yield and gas composition from the pyrolysis–catalytic steam reforming of biomass with the nickel-ash-based catalysts

Sample	Sand	Nickel-tyre ash	Nickel-coal ash	Nickel-RDF ash
Gas yield (wt%)	39.9	59.3	54.9	58.03
Gas composition (vol%)				
CO	43.50	34.64	39.40	33.60
CO <sub>2</sub>	14.10	15.19	14.07	17.30
H <sub>2</sub>	19.92	35.79	28.51	34.40
CH <sub>4</sub>	15.33	10.00	12.78	10.60
C <sub>2</sub> H <sub>4</sub>	7.15	4.37	5.25	4.20
H <sub>2</sub> yield (mmol g <sup>-1</sup> biomass)	3.39	10.50	7.29	9.66

Zn-free commercial alumina. Alkali metals (K<sub>2</sub>O, Na<sub>2</sub>O) were also identified in the different waste ashes (Table 1) used in this study. Sodium and potassium compounds have also been reported as catalysts for hydrocarbon decomposition and improved gas quality [21]. It has been suggested that the presence of alkali metal compounds act as catalysts to increase hydrocarbon cracking and reforming and thereby increase hydrogen production from biomass [20, 26].

The wide range of metal and alkali metal catalysts present in the combustion ash samples will clearly have a catalytic effect on the catalytic steam reforming, dry reforming, thermal cracking and gasification reactions involving the evolved biomass pyrolysis gases. Other researchers have investigated the use of combustion ashes and reported a catalytic effect. Wang et al. [16] used a combustion ash produced from coal as a catalyst for the catalytic steam reforming of acetic acid and phenol and compared their results with several commonly used steam-reforming catalysts. They showed that the coal ash sample produced similar carbon conversion efficiencies and hydrogen for acetic acid to that of an Fe–Al<sub>2</sub>O<sub>3</sub> catalyst. For phenol, the results were lower in terms of conversion and H<sub>2</sub> yield.

### Pyrolysis–catalytic steam reforming of biomass with nickel-ash catalysts

Table 4 shows the influence of the addition of 10 wt% nickel to the combustion ash catalysts in terms of gas yield and gas composition derived from the pyrolysis–catalytic steam reforming of biomass. In addition, comparison is again made with the yields in relation to no-catalyst (in the presence of quartz sand). There was only a small influence of nickel addition to the combustion ashes in terms of any increase in total gas yield compared to the non-nickel-impregnated combustion ash samples shown in Table 3. For example, the total gas yield increased by 6.6 wt% for the Ni-tyre ash, 4.6 wt% for the Ni-coal ash sample, whilst the Ni-RDF ash sample showed a similar total gas yield compared to the ash-only catalysts. However, the hydrogen yield in relation to the mass of biomass feedstock showed a significant increase for all the nickel-impregnated ash catalysts. For example the

Ni-tyre ash catalyst increased the hydrogen yield to produce the highest yield  $10.5 \text{ mmol}^{-1} \text{ H}_2$  from the biomass. The presence of the nickel in the ash catalysts showed that nickel metal catalytic steam reforming of the hydrocarbons ( $\text{CH}_4$  and  $\text{C}_2\text{--H}_4$ ) occurred, producing increased hydrogen yield in terms of  $\text{H}_2$  yield as  $\text{mmol g}^{-1}_{\text{biomass}}$  and also a volumetric increase in hydrogen content in the gas product. The results suggest that the high metal content of the combustion ashes acts as the main catalytic effect and that addition of a further active nickel content to the catalyst produces an approximate 20% increase in hydrogen yield.

The addition of nickel to combustion ash to enhance the catalytic effect of the metals and compounds in the ash has been examined by other researchers. For example, Wang et al. [16] investigated the catalytic steam reforming of bio-oil model compounds in the form of acetic acid and phenol using a nickel-coal ash catalyst with a 15 wt% nickel loading. The conversion of acetic acid was 57.5% and for phenol conversion was 26.3% with the combustion ash, but increased to 98.4% and 83.5%, respectively, with the nickel-ash catalyst. In addition, they reported that the yield of  $\text{H}_2$  from the catalytic steam reforming of acetic acid using the combustion ash was 50.2% and for phenol was 19.6%. However, with the addition of nickel to the ash, the yield of  $\text{H}_2$  improved to 85.6% for acetic acid and 79.1% for phenol at a catalyst temperature of  $700 \text{ }^\circ\text{C}$  and steam/carbon ratio of 9.2. The influence of temperature was to increase the conversion of the bio-oil model compounds and increase hydrogen yield. In a later report, Wang et al. [2] added both nickel and iron to a coal combustion ash to produce a Ni-Fe-ash catalyst for the catalytic steam reforming of acetic acid. They reported 100% conversion of the acetic acid and a hydrogen yield of 89.6% at a catalyst temperature of  $700 \text{ }^\circ\text{C}$ .

## Conclusions

The work reported here has shown the potential of combustion ash produced from coal, municipal solid waste and tyres have the potential to be used as catalysts for the catalytic steam reforming of biomass. The process used a pyrolysis-catalytic steam reforming experimental system with the ashes as catalyst. Combustion ashes produced from coal, RDF and waste tyres have been shown to contain a high metal content which have been used as catalysts for the production of a hydrogen-rich gas from waste biomass. The results showed that total gas and  $\text{H}_2$  yield were significantly increased in the presence of the combustion ash catalysts. The  $\text{H}_2$  yields produced from biomass in the presence of the ash catalysts were  $7.90 \text{ mmol g}^{-1}_{\text{biomass}}$  with the RDF-derived ash (29.73 vol%  $\text{H}_2$ ),  $6.54 \text{ mmol g}^{-1}_{\text{biomass}}$  (27.98 vol%) with the tyre rubber ash and  $4.79 \text{ mmol g}^{-1}_{\text{biomass}}$  (22.08 vol%) with the coal ash catalyst. Addition of nickel

to the combustion ash samples showed a further significant increase of  $\sim 20\%$  in the yield of hydrogen.

The ashes contained  $\text{Al}_2\text{O}_3$ ,  $\text{CaO}$ ,  $\text{MgO}$ , and  $\text{Fe}_2\text{O}_3$  which have been used in the catalytic steam reforming of biomass. In addition, the ashes contain metals such as Mg, Zn and Cu which have been used as catalyst promoters in steam-reforming catalysts and  $\text{K}_2\text{O}$ ,  $\text{Na}_2\text{O}$  which have been used as catalysts for hydrocarbon cracking and reforming. However, it is difficult to assign particular metals present in the ashes for the catalytic effect on hydrogen production from biomass. For example, the ash samples contained mixtures of metals and metal species which would contribute to the catalytic activity of the ashes and also would have had a synergistic or promotional effect on enhancing hydrogen production from the biomass. Combustion ashes are regarded as problematic wastes with low commercial value and often are disposed of in waste landfill sites, representing a waste of resource. This work has identified combustion ashes as a potentially useful and low cost catalyst for catalytic steam reforming of biomass pyrolysis gases.

**Open Access** This article is distributed under the terms of the Creative Commons Attribution 4.0 International License (<http://creativecommons.org/licenses/by/4.0/>), which permits unrestricted use, distribution, and reproduction in any medium, provided you give appropriate credit to the original author(s) and the source, provide a link to the Creative Commons license, and indicate if changes were made.

## References

1. Reijnders L (2005) Disposal, use and treatments of combustion ashes: a review. *Resour Conserv Recycl* 43:313–336
2. Wang S, Zhang F, Cai Q, Zhu L, Luo Z (2015) Steam reforming of acetic acid over coal ash supported Fe and Ni catalysts. *Int J Hydrog Energy* 40:11406–11413
3. Feuerborn HJ (2011) Coal combustion products in Europe—an update on production and utilisation, standardisation and regulation. World of Ash Conference, Denver, CO, USA, 9–11 May
4. CEWEP (2018) Confederation of European waste-to-energy plants, Bottom Ash Factsheet, CEWEP, Brussels, Belgium
5. Ashish DK, Verma SK, Singh J, Sharma N (2018) Strength and durability characteristics of bricks made using coal bottom and coal fly ash. *Adv Concr Constr* 6:407–422
6. Rafeizonooz M, Mirza J, Salim MR, Hussin MW, Khankhaje E (2016) Investigation of coal bottom ash and fly ash in concrete as replacement for sand and cement. *Constr Build Mater* 116:15–24
7. Argiz C, Sanjuan MA, Menendez E (2017) Coal bottom ash for Portland cement production. *Adv Mater Sci Eng*. ID6068286
8. Chuang KH, Lu CH, Chen JC, Wey MY (2018) Reuse of bottom ash and fly ash from mechanical-bed and fluidized-bed municipal incinerators in manufacturing lightweight aggregates. *Ceram Int* 44:12691–12696
9. Romeo E, Mantovani L, Mario Tribaudino M, Montepara A (2018) Reuse of stabilized municipal solid waste incinerator fly ash in asphalt mixtures. *J Mater Civ Eng* 30:04018157

10. Yang Z, Tian S, Liu L, Wang X, Zhang Z (2018) Application of washed MSWI fly ash in cement composites: long-term environmental impacts. *Environ Sci Poll Res* 25:12127–12138
11. Goodarzi F (2006) Characteristics and composition of flyash from Canadian coal-fired power plants. *Fuel* 85:1418–1427
12. Lynn CJ, Ghataora GS, Dhir RK (2017) Municipal incinerated bottom ash (MIBA) characteristics and potential for use in road pavements. *Int J Pavement Res Technol* 10:185–201
13. Pfranf-Stotz G, Reichelt J (1997) Characterisation and valuation of municipal solid waste incineration bottom ashes. In: 1st international symposium on incineration and flue gas treatment technologies, Sheffield, UK, July
14. Evans J, Williams PT (2000) Heavy metal adsorption onto flyash in waste incineration flue gases. *Trans I Chem E* 78:40–46
15. Singh S, Nimmo W, Williams PT (2013) An experimental study of ash behaviour and the potential fate of ZnO/Zn in the Co-combustion of pulverised South African coal and waste tyre rubber. *Fuel* 111:269–279
16. Wang S, Zhang F, Cai Q, Li X, Zhu L, Wang Q, Luo Z (2014) Catalytic steam reforming of bio-oil model compounds for hydrogen production over coal ash supported Ni catalyst. *Int J Hydrog Energy* 39:2018–2025
17. Shahbaz M, Yusup S, Inayat A, Patrick DO, Pratama A, Ammar M (2017) Optimization of hydrogen and syngas production from PKS gasification by using coal bottom ash. *Bioresour Technol* 241:284–295
18. Loy ACM, Yusup S, Lam MK, Chin BLF, Shabaz M, Yamamoto A, Acda MN (2018) The effect of industrial waste coal bottom ash as catalyst in catalytic pyrolysis of rice husk for syngas production. *Energy Convers Manag* 165:541–554
19. Huang Q, Lu P, Hu B, Chi Y, Yan J (2016) Cracking of model tar species from the gasification of municipal solid waste using commercial and waste-derived catalysts. *Energy Fuel* 30:5740–5748
20. Huang Z, He F, Zhu H, Chen D, Zhao K, Wei G, Feng Y, Zheng A, Zhao Z, Li H (2015) Thermodynamic analysis and thermogravimetric investigation on chemical looping gasification of biomass char under different atmospheres with Fe<sub>2</sub>O<sub>3</sub> oxygen carrier. *Appl Energy* 157:546–553
21. Shahbaz M, Yusup S, Inayat A, Patrick DO, Ammar M (2017) The influence of catalysts in biomass steam gasification and catalytic potential of coal bottom ash in biomass steam gasification: a review. *Renew Sustain Energy Rev* 73:468–476
22. Garcia L, French R, Czernik S, Chornet E (2000) Catalytic steam reforming of bio-oils for the production of hydrogen: effects of catalyst composition. *Appl Catal A-Gen* 201:225–239
23. Garcia L, Benedicto A, Romeo E, Salvador ML, Arauzo J, Bilbao R (2002) Hydrogen production by steam gasification of biomass using Ni–Al co-precipitated catalysts promoted with magnesium. *Energy Fuel* 16:1222–1230
24. Li Y, Chen J, Qin Y, Chang L (2000) Simultaneous production of hydrogen and nanocarbon from decomposition of methane on a nickel-based catalyst. *Energy Fuel* 14:1188–1194
25. Dong L, Wu C, Ling H, Shi J, Williams PT, Huang J (2017) Promoting hydrogen production and minimizing catalyst deactivation from the pyrolysis-catalytic steam reforming of biomass on nanosized NiZnAlOx catalysts. *Fuel* 188:610–620
26. Li J, Yin Y, Zhang X, Liu J, Yan R (2009) Hydrogen-rich gas production by steam gasification of palm oil wastes over supported tri-metallic catalyst. *Int J Hydrog Energy* 34:9108–9115

**Publisher's Note** Springer Nature remains neutral with regard to jurisdictional claims in published maps and institutional affiliations.